HHS Public Access

Author manuscript

J Physiol. Author manuscript; available in PMC 2021 April 07.

Published in final edited form as:

J Physiol. 2019 June ; 597(11): 2887–2901. doi:10.1113/JP277580.

Studies into the determinants of skeletal muscle oxygen consumption: novel insight from near-infrared diffuse correlation spectroscopy

Wesley J. Tucker[1,2], **Ryan Rosenberry**[1], **Darian Trojacek**[1], **Houda H. Chamseddine**[1], **Carrie A. Arena-Marshall**[2], **Ye Zhu**[3], **Jing Wang**[2], **J. Mikhail Kellawan**[4], **Mark J. Haykowsky**[2], **Fenghua Tian**[3], **Michael D. Nelson**[1,3]

[1]Department of Kinesiology, University of Texas at Arlington, Arlington, TX, USA

[2]College of Nursing, University of Texas at Arlington, Arlington, TX, USA

[3]Department of Bioengineering, University of Texas at Arlington, Arlington, TX, USA

[4]Department of Health and Exercise Science, University of Oklahoma, Norman, OK, USA

Abstract

Diffuse correlation spectroscopy (DCS) is emerging as a powerful tool to assess skeletal muscle perfusion. Combining DCS with near-infrared spectroscopy (NIRS) introduces exciting possibilities for understanding the determinants of muscle oxygen consumption; however, no investigation has directly compared NIRS–DCS to conventional measures of oxygen delivery and utilization in an exercising limb. To address this knowledge gap, nine healthy males performed rhythmic handgrip exercise with simultaneous measurements by NIRS–DCS, Doppler blood flow and venous oxygen content. The two approaches showed good concurrent validity, with directionally similar responses between: (a) Doppler-derived forearm blood flow and DCS-derived blood flow index (BFI), and (b) venous oxygen saturation and NIRS-derived tissue saturation. To explore the utility of combined NIRS–DCS across the physiological spectrum, we manipulated forearm arterial perfusion pressure by altering the arm position above or below the level of the heart. As expected, Doppler-derived skeletal muscle blood flow increased with exercise in both arm positions, but with markedly different magnitudes (below: +424.3 ± 41.4 ml/min, above: +306 ± 12.0 ml/min, $P = 0.002$). In contrast, DCS-derived microvascular BFI increased to a similar extent with exercise, regardless of arm position ($P = 0.65$). Importantly, however, the time to reach BFI steady state was markedly slower with the arm above the heart, supporting the experimental

Corresponding author M. D. Nelson: Department of Kinesiology, University of Texas at Arlington, Science & Engineering Innovation & Research Building, 701 S. Nedderman Drive, Room 105, Arlington, TX 76019, USA. michael.nelson3@uta.edu.

Author contributions

This work was done in the Potratz Family Applied Physiology and Advanced Imaging Laboratory at the University of Texas at Arlington. Authors W.J.T., R.R., D.T., M.J.H., F.T. and M.D.N. contributed to the conception and design of the work; W.J.T., R.R., D.T., H.H.C., C.A.A.-M., Y.Z., J.W., J.M.K., M.J.H., F.T. and M.D.N. contributed to acquisition, analysis or interpretation of data; and W.J.T., R.R., D.T., H.H.C., C.A.A.-M., Y.Z., J.W., J.M.K., M.J.H., F.T. and M.D.N. contributed to drafting the work or revising it critically for important intellectual content. All authors have read and approved the final version of this manuscript and agree to be accountable for all aspects of the work in ensuring that questions related to the accuracy or integrity of any part of the work are appropriately investigated and resolved. All persons designated as authors qualify for authorship, and all those who qualify for authorship are listed

Competing interests

The authors have no conflicts of interest to report.

design. Notably, we observed faster tissue desaturation at the onset of exercise with the arm above the heart, resulting in similar muscle oxygen consumption profiles throughout exercise. Taken together, these data support a novel role for NIRS–DCS in understanding the determinants of skeletal muscle oxygen utilization non-invasively and throughout exercise.

Introduction

Diffuse correlation spectroscopy (DCS) is emerging as a powerful new tool to assess skeletal muscle perfusion (Gurley *et al.* 2012; Henry *et al.* 2015; Baker *et al.* 2017; Carp *et al.* 2017; Shang *et al.* 2017; Bangalore-Yogananda *et al.* 2018; Hammer *et al.* 2018). DCS is completely non-invasive, has excellent temporal resolution (Bi *et al.* 2015) and has been validated in a variety of organs and tissues against several different standards, including laser Doppler (Shang *et al.* 2011), xenon-CT (Kim *et al.* 2014), fluorescent microsphere flow measurements (Zhou *et al.* 2009) and arterial spin labelled-MRI (Yu *et al.* 2007).

Combining DCS with conventional near-infrared spectroscopy (NIRS) – an established technique for characterizing the transport and utilization of oxygen through the microcirculation (Belardinelli *et al.* 1995; DeLorey *et al.* 2003, 2004; Grassi *et al.* 2003; Ferreira *et al.* 2005; Broxterman *et al.* 2014, 2015; Koga *et al.* 2014; Grassi & Quaresima,2016;Sun *etal.* 2016;Barstow,2019)–introduces exciting new possibilities for understanding the determinants of muscle oxygen utilization at the microvascular level. Several laboratories have already combined DCS with conventional NIRS during exercise, establishing good ‘proof-of-concept’ (Henry *et al.* 2015; Baker *et al.* 2017; Carp *et al.* 2017; Hammer *et al.* 2018); however, none of these prior investigations have directly compared NIRS–DCS to conventional Fick determinants of oxygen delivery (i.e. bulk skeletal muscle blood flow) and utilization (i.e. fractional oxygen extraction). Moreover, none of these investigations attempted to manipulate the balance between oxygen delivery and utilization in an effort to explore the utility of NIRS–DCS across the physiological spectrum. Establishing the utility of this device could indeed have a major impact, both mechanistically and therapeutically, in healthy and clinical populations.

To address these knowledge gaps, we constructed a dual-wavelength combined NIRS–DCS device to simultaneously measure skeletal muscle oxygen delivery (i.e. tissue perfusion) and utilization (i.e. tissue saturation). With this device, we first tested the hypothesis that NIRS–DCS-derived indices of skeletal muscle oxygen delivery and utilization would be closely related to conventional Fick equivalents (i.e. Doppler-derived muscle blood flow and venous oxygen content, respectively) during rhythmic handgrip exercise. Then, to manipulate convective oxygen delivery to skeletal muscle, forearm arterial perfusion pressure was experimentally reduced or increased by changing the position of the exercising arm above or below the level of the heart, respectively (Saunders & Tschakovsky, 2004; Tschakovsky *et al.* 2004; Walker *et al.* 2007; Bentley *et al.* 2014; Jasperse *et al.* 2015). Given that skeletal muscle blood flow tracks changes in perfusion pressure, we hypothesized that skeletal muscle oxygen utilization (Fick-derived and NIRS–DCS-derived) would change in opposition to delivery in order to maintain oxygen consumption.

Methods

Ethical approval and subjects

The study was approved by the Institutional Review Board for research involving Human Subjects at the University of Texas at Arlington and conformed to the *Declaration of Helsinki*. All subjects provided signed consent after receiving a complete verbal and written description of the experimental protocol and potential risks. The study was not registered in a database.

Subject recruitment was limited to young recreationally active males (18–35 years old). Exclusion criteria included: body mass index (BMI) <18.5 or >35 kg/m^2, handgrip maximal voluntary contraction (MVC) <40 kg or >65 kg, history of cardiovascular, pulmonary or metabolic disease, uncontrolled hypertension, significant anaemia (haemoglobin <8 g/dl), current medication or tobacco use, orthopedic limitations, poor venous access and poor acoustic window capacity for brachial artery imaging by ultrasound.

Experimental design

Screening and familiarization.—All subjects came to the laboratory for an initial screening and familiarization visit. Subjects who met the inclusion/exclusion criteria were then fully instrumented (with the exception of a retrograde catheter) and asked to perform each of the experimental conditions that would be performed during the main experimental testing day. Subjects also underwent dual-energy X-ray absorptiometry to quantify fat/lean mass.

Experimental testing visit.—Experimental testing visits were performed on a separate day, after the initial screening/familiarization visit. All studies were performed in a quiet, temperature- (~22°C) and ambient light-controlled room. Subjects were studied in a fasted state, having abstained from alcohol and vigorous exercise for >24 h, and caffeine for >12 h. Upon arrival at the laboratory, subjects were positioned supine on a bed and asked to rest quietly while a retrograde I.V. catheter was inserted into a deep vein in the forearm of the exercising (non-dominant) arm. Subjects were then instrumented for measurement of continuous blood pressure, heart rate, arterial oxygen saturation, brachial blood flow and skeletal muscle oxygen delivery/utilization (described in detail below). A Smedley handgrip dynamometer (Stoelting Company, Wood Dale, IL, USA) was positioned next to the subject's exercising arm, so that the arm could comfortably be extended and supported. Once fully instrumented, subjects completed the following experimental aims.

Experimental Aim 1.: To test whether our combined NIRS–DCS device is closely related to Fick equivalents (i.e. Doppler-derived muscle blood flow and venous oxygen content, respectively), subjects performed 4 min of rhythmic handgrip exercise at 13 kg using a 50% contraction duty cycle (2 s contraction, 2 s relaxation) at a rate of 15 contractions per minute, with simultaneous measurements of oxygen delivery and utilization by both approaches (Fick-derived and NIRS–DCS-derived). Exercise was guided by a monitor that displayed the handgrip force output to give the subject visual feedback on force production, and a recorded voice prompt to guide contraction/relaxation.

Experimental Aim 2.: To manipulate oxygen delivery to skeletal muscle, forearm perfusion pressure was experimentally reduced or increased by changing the position of the exercising arm above or below the level of the heart, respectively (Saunders & Tschakovsky, 2004; Tschakovsky *et al.* 2004; Walker *et al.* 2007; Bentley *et al.* 2014; Jasperse *et al.* 2015). The order of the arm position (above *versus* below) was randomized between subjects, and each condition was separated by a minimum of 20 min. Subjects were instrumented as described in the neutral position, with the exercise and data monitoring held constant as well.

Instrumentation and measurements

Anthropometrics and habitual physical activity levels.—Dual-energy X-ray absorptiometry (DXA) was used to determine whole-body body fat percentage, fat mass and fat-free mass (DXA, Lunar Prodigy, GE Healthcare, Little Chalfont, UK). A DXA-certified radiology technician also constructed a region-of-interest from the left arm antecubital fossa through the fingertips on the left hand to quantify forearm lean mass. Height and weight were measured with a dual-function stadiometer and weighing scale (Professional 500KL, Health-O-Meter, McCook, IL, USA). Forearm adipose tissue thickness was measured with skinfold calipers (Slim Guide, Creative Health Systems, Plymouth, MI, USA) on the left arm at the location of the flexor digitorum profundus. Self-reported habitual physical activity levels were quantified with the validated Stanford Leisure-Time Activity Categorical Item survey (L-Cat, Version 2.2) (Kiernan *et al.* 2013; Ross *et al.* 2018).

Central haemodynamic responses.—Beat-by-beat arterial blood pressure was measured from a small finger cuff placed around the middle finger of the subject's non-exercising hand using photoplethysmography (Finometer PRO, Finapres Medical Systems, Arnhem, The Netherlands) that was calibrated to an automated brachial artery blood pressure cuff (Connex Spot Monitor, Model 71WX-B, Welch Allyn, Skaneateles Falls, NY, USA). Mean arterial blood pressure (MAP) was calculated as the mean pressure across a continuous average of arterial waveforms (1 min average for resting baseline and 30 s average during exercise). Heart rate was measured via three-lead electro-cardiography (ECG) using standard CM_5 placement of ECG electrodes (MLA 0313; ADInstruments, Colorado Springs, CO, USA). Arterial oxygen saturation (S_{aO_2}) was non-invasively obtained by placing a pulse oximeter (ML 320; ADInstruments) over the index finger of the subject's non-exercising hand. The analog outputs for arterial blood pressure, heart rate and S_{aO_2} modules were connected to a high-performance, physiological data acquisition system (PowerLab 16/35, ADInstruments) for simultaneous data recording.

Forearm blood flow.—Brachial artery blood flow velocity and diameter were measured with a duplex ultrasound system (Vivid-i, GE Healthcare) on the upper left portion of the exercising arm (proximal to the antecubital fossa). This ultrasound system had a 12 MHz linear array probe with 60 degrees of insonation. The ultrasound gate was optimized to ensure complete insonation of the entire vessel cross-section with constant intensity. The continuous Doppler audio signal was converted to real-time blood flow velocity waveforms using a validated Doppler audio converter (Herr *et al.* 2010) and recorded using a PowerLab data acquisition system (ADInstruments). Brachial artery diameter was measured with B-

mode ultrasound imaging, with measurements made during the resting baseline and during the final 30 s of rhythmic handgrip exercise. The analog outputs from the Doppler ultrasound module along with the amplified signal from the handgrip dynamometer were connected to the data acquisition system detailed above for simultaneous data recording.

Forearm deep venous blood sampling.—An 18-gauge I.V. catheter was inserted retrograde to venous blood flow into a deep forearm vein. Confirmation that the selected vein drained from the active muscle group of interest (flexor digitorum profundus) was obtained using ultrasound and/or a portable vein illuminator imaging device (VeinViewer Flex, Christie Medical Holdings Inc., Memphis, TN, USA) prior to insertion of the catheter. This provided blood samples of venous effluent draining directly from the exercising muscle with little contamination from the surrounding inactive tissue. Blood samples were taken during the resting baseline and during the final 30 s of each exercise bout to measure venous oxygen content (C_{vO_2}). A 3 ml discard was drawn prior to the 2 ml blood sample. A 2 ml saline flush followed each sample to prevent the catheter from clotting.

Near-infrared spectroscopy and diffuse correlation spectroscopy

A dual-wavelength NIRS–DCS combined system was built in-house and used to simultaneously measure changes in skeletal muscle perfusion and oxygenation during handgrip exercise. The system consists of two continuous-wave, long coherence-length laser diodes (785 nm and 852 nm, Crystalaser Inc., Reno, NV, USA) as the light sources that are alternately switched (MEMS 2 × 2 Blocking Switch, Dicon Fiberoptics Inc., Richmond, CA, USA), and a single-photon-counting avalanche photodiode (APD) as the photon detector (SPCM-AQRH-14-FC, Pacer USA LLC., Palm Beach Gardens, FL, USA). The output of the APD is connected to a computer with a 32-bit, 8-channel data acquisition card (PCI-6602, National Instruments Corp., Austin, TX, USA). A LabVIEW (National Instruments Corp.) program was developed for photon counting. A software autocorrelator calculates the autocorrelation function and absolute intensity (sum of photon counts) of diffused light, which reduced overall cost and complexity of the system as compared with a hardware autocorrelator (Dong *et al.* 2012). A 3-D-printed probe was used to hold a multi-mode fibre (125 μm in core diameter) from the optical switch and a single-mode fibre (5 μm in core diameter) to the APD detector. The probe was affixed to the forearm of the exercise arm, directly over the belly of the flexor digitorum profundus, using black Velcro strips. The belly of the flexor digitroum profundus was located by careful tissue palpations. The source-to-detector distance was 2.5 cm. The data sampling rate was 0.25 Hz.

DCS measurements.—A detailed description of DCS methods is outlined in a previous report (Bangalore-Yogananda *et al.* 2018). Briefly, DCS determines a blood flow index (BFI) based on the autocorrelation function of light reflectance. In this study, BFI was measured at each of the two near-infrared wavelengths (785 nm and 852 nm), which produced nearly identical responses. Accordingly, BFI is reported as the average of both signals. Then, relative muscle blood flow (%) from the initial baseline at t_0, rMBF, was calculated as:

$$\mathrm{rMBF} = \frac{\mathrm{BFI}(t)}{\mathrm{BFI}(t_0)}100 \tag{1}$$

NIRS measurements.—The absolute intensity of light reflectance can be used to determine the haemoglobin concentrations based on conventional NIRS methods. First, the absolute light intensity measured at each wavelength over time, $I(t)$, was converted to the changes in optical density, ΔOD, which is given as:

$$\Delta\mathrm{OD} = \log_{10}[I(t_0)/(t)] \tag{2}$$

Then two ΔOD outputs measured at 785 nm and 852 nm, respectively, were used to quantify the relative changes in oxygenated haemoglobin (HbO_2) and deoxygenated haemoglobin (Hb) concentrations, $\Delta HbO_2(t)$ and $\Delta Hb(t)$, based on the modified Beer–Lambert Law (Cope *et al.* 1988). Finally, the change in total haemoglobin concentration was derived as:

$$\Delta\mathrm{HbT}(t) = \Delta\mathrm{HbO}_2(t) + \Delta\mathrm{Hb}(t) \tag{3}$$

It is noted that conventional NIRS only quantifies the relative changes in haemoglobin concentrations from an initial baseline. In this study, the haemoglobin baseline values, namely $HbO_2(t_0)$, $Hb(t_0)$ and $HbT(t_0)$, were measured prior to the experiment in each arm position with a frequency-domain near-infrared tissue oximeter (OxiplexTS, ISS Inc., Champaign, IL, USA) and then kept constant. Therefore, the real-time absolute haemoglobin concentrations were derived as:

$$\begin{aligned}\mathrm{HbO}_2(t) &= \mathrm{HbO}_2(t_0) + \Delta\mathrm{HbO}_2(t)\\ \mathrm{Hb}(t) &= \mathrm{Hb}(t_0) + \Delta\mathrm{Hb}(t)\\ \mathrm{HbT}(t) &= \mathrm{HbT}(t_0) + \Delta\mathrm{HbT}(t)\end{aligned} \tag{4}$$

Further, the real-time tissue oxygen saturation (%) was derived as:

$$\mathrm{S}_{\mathrm{tO}_2}(t) = \frac{\mathrm{HbO}_2(t)}{\mathrm{HbO}_2(t) + \mathrm{Hb}(t)} \times 100 \tag{5}$$

Metabolic rate of oxygen.—By combining the $\Delta[HbO_2]$ and $\Delta[Hb]$ changes from NIRS, and the rMBF change from DCS, the relative change of skeletal muscle metabolic rate of oxygen, MRO_2, can be calculated as (Boas *et al.* 2003):

$$\mathrm{MRO}_2 = \mathrm{rMBF}\left(1 + \frac{\Delta\mathrm{Hb}(t)}{\mathrm{Hb}(t_0)}\right)\left(1 + \frac{\Delta\mathrm{HbT}(t)}{\mathrm{HbT}(t_0)}\right)^{-1} \tag{6}$$

Altering forearm arterial perfusion pressure

To manipulate blood flow to forearm skeletal muscle we positioned the arm above or below the level of the heart to alter forearm arterial perfusion pressure (FAPP). This experimental setup has been shown to create a local FAPP difference between the arm placed above *versus* below the level of the heart (Saunders & Tschakovsky, 2004; Bentley *et al.* 2014). The exercising arm was raised or lowered and allowed to rest against a wooden board that was held in place with an industrial-sized rotating clamp (Jawstand, Rockwell Tools, Charlotte, NC, USA). To assess the difference in FAPP between arm positions, we non-invasively measured resting arterial blood pressure using a servo-controlled finger photoplethysmography (Human NIBP Controller, ADInstruments) that was placed on the middle or index finger of the left hand of the manipulated arm. Finger arterial blood pressure waveforms were recorded after the arm rested for 10 min in each arm position (neutral, arm above the heart, arm below the heart). FAPP was then determined by adding or subtracting the pressure equivalent in mmHg of the measured hydrostatic column (mid-forearm to heart level), associated with arm-above or arm-below-heart positions, from the blood pressure measured continuously at heart level (Walker *et al.* 2007; Bentley *et al.* 2014).

Data analysis

Doppler ultrasound, arterial blood pressure, heart rate and DCS-NIRS-derived variables were measured throughout rest, exercise and post-exercise recovery. To minimize muscle fibre motion artifact during exercise, DCS-NIRS data were recorded only during the relaxation phase of the handgrip duty cycle, as previously described (Gurley *et al.* 2012; Bangalore-Yogananda *et al.* 2018). Accordingly, brachial artery blood flow measurements were also made during the relaxation phase of the handgrip duty cycle, to match DCS. Venous blood sampling was limited to a single resting baseline and end-exercise measurement. With the exception of data presented continuously in figures, resting baseline values represent a 1 min average of the final minute of a 2 min baseline, and exercise values represent the first 30 s of the final minute of a 4 min exercise bout. We purposefully avoided the final 30 s of exercise as this period was sometimes associated with motion artifact from the blood draw and/or artifact from the subsequent saline flush.

Venous blood constituents.—An I-STAT analyser (I-STAT 1, Abbott Point of Care, Princeton, NJ, USA) was used to analyse the whole blood sample for haemoglobin and forearm venous oxygen saturation (S_{vO_2}) using CG8+ test cartridges (Abbott Point of Care). All blood samples were analysed in duplicate, and averaged.

Calculated physiological variables.—Doppler ultrasound, arterial blood pressure, heart rate and S_{aO_2} data were analysed offline by a single observer (W.J.T.) using the LabChart Pro software environment (ADInstruments). For real-time arterial blood pressure waveforms, a peak-detection algorithm was applied to identify the systolic and diastolic components as the peak and valley of each arterial wave. Then mean arterial pressure (MAP, mmHg) was calculated on a beat-to-beat basis. Similarly, mean blood flow velocity (MBV, cm/s) was calculated as the beat-to-beat average from the real-time Doppler ultrasound waveforms. Forearm brachial artery blood flow (FBF) was estimated as [MBV × π(brachial

artery diameter/2)^2] × 60, where brachial artery diameter (cm) was measured with B-mode ultrasound imaging. FBF was indexed to lean forearm mass and reported as millilitres per minute per 100 g lean forearm tissue. Forearm vascular conductance was calculated as FBF/MAP × 100. Arterial oxygen content (C_{aO_2}) was calculated as [(S_{aO_2} × [Hb] × 1.36) + 0.003 × P_{aO_2}]. P_{aO_2} is the partial pressure of O_2 in arterial blood and was assumed to be 100 mmHg. Venous blood samples were used to calculate venous oxygen content (C_{vO_2}) using Formula [(S_{vO_2} × [Hb] × 1.36) + 0.003 × P_{vO_2}], where S_{vO_2} is venous oxygen saturation and P_{vO_2} is the partial pressure of oxygen in venous blood. Skeletal muscle oxygen uptake ($m\dot{V}_{O_2}$) was calculated using the Fick equation: $\text{FBF} \times \left(C_{aO_2} - C_{vO_2}\right)$. Oxygen delivery was calculated as $\text{FBF} \times C_{aO_2}$.

NIRS and DCS.—All raw DCS and NIRS data were analysed in MATLAB (Version R2016A, MathWorks Inc., Natick, MA, USA) and exported to Microsoft Excel (Microsoft Corporation, Redmond, WA, USA) for subsequent statistical analyses.

Statistics

All statistical analyses were performed with SPSS Software (SPSS 24.0, IBM Corp., Armonk, NY, USA) and Prism version 8 (GraphPad Software, La Jolla, CA, USA). For all statistical tests, significance was accepted at $P < 0.05$. All data are presented as means ± SEM, unless otherwise noted. Prior to analysis, normality distribution was examined for all variables using the Shapiro–Wilk test.

For Experimental Aim 1, a one-way repeated measures analysis of variance (ANOVA) was used to test for differences between resting and exercise values for all physiological and NIRS–DCS-derived variables. For Experimental Aim 2, a two-way repeated measures ANOVA was used to test for main effects of time (rest *versus* exercise) and condition (arm above *versus* below the level of the heart) as well as an interaction effect for all physiological and NIRS–DCS-derived variables. For all repeated measures ANOVA testing, if the sphericity assumption was violated (Greenhouse–Geisser $\varepsilon < 0.75$), degrees of freedom (d.f. values) were adjusted using the Greenhouse–Geisser correction. When significant overall effects were observed, a Bonferroni correction *post hoc* analysis was performed to determine where significant differences existed.

To quantify and compare the responses over time between the conventional and NIRS–DCS approaches (Aims 1 and 2), a monoexponential model (Grassi *et al.* 2003) using curve fitting was fitted to the time series data. For an uphill curve with an upward trend in the response (FBF, BFI and MRO_2) over time, the model function was written as:

$$Y = Y_0 + A(1 - \exp(-(t - t_0)/\tau)) \quad (7)$$

where Y is the increase of the response at time t above that at rest, Y_0 is the baseline value at time t=0 at rest, t_0 is the time at which the increase or decrease begins, representing an early delay-like phase (Phase 1 during 0–1 min), followed by an exponential increase in the response (Phase 2 during 1–2 min) and a steady state (Phase 3 during 2–5 min), A is the

amplitude between Y_0 and the steady-state value of Y, and τ is the time constant, representing the amount of time that it takes to change 63% of the steady-state amplitude. As described by Grassi *et al.* (2003), these three phases of the response reflect the underlying physiology of the transient phase. The parameters in the above equation are estimated by minimizing the sum of squares residuals. Similarly, for a downhill curve with downward trend in the response (tissue saturation) over time, the model function was written as:

$$Y = (Y_0 - A) + A \exp(-(t - t_0)/\tau)) \quad (8)$$

where Y is the decrease of the response at time t below that at rest, and A is the amplitude between Y_0 and the steady-state value ($Y_0 - A$). Given $t_0 = 1$, it should be noted that the shape of the curve was solely determined by the time constant (τ), if applicable, and therefore the two approaches were compared in terms of τ when applicable. In addition, the exponential model was not applicable to S_{vO_2} and $m\dot{V}_{O_2}$ since they were measured at only two time points (baseline and exercise). For these two responses, the meaningful comparison between the two approaches was based on the direction of the trend in the response over time.

Results

Nineteen subjects volunteered to participate in the study. Four subjects were excluded from participation during the screening/familiarization visit due to a poor acoustic brachial artery imaging window. Fifteen subjects completed all testing visits; however, six of these subjects were excluded from the final analysis due to technical difficulties ($n = 3$) or poor data quality ($n = 3$). The results for Experimental Aim 1 are reported on the remaining nine subjects (subject descriptives in Table 1). For Experimental Aim 2, we were unable to obtain blood in the above condition in one subject. As such, eight subjects were included in the analysis for Experimental Aim 2.

Experimental Aim 1

Forearm blood flow and tissue perfusion.—Conventional measures of FBF and oxygen delivery significantly increased with handgrip exercise (Fig. 1A, Table 2), with DCS-derived blood flow index (BFI) sharing a similar response (Fig. 1B). There was good agreement in parameter estimates from the non-linear regression models between FBF and BFI, with τ values of 25.0 s and 26.1 s, respectively. There was also large overlap in their associated 95% confidence intervals 23.1–31.6 s and 15.8–40.0 s, indicating these parameters were not likely to be significantly different from each other. To explore this relationship further, a subset of individuals ($n = 4$) returned for a separate visit to perform an incremental handgrip test at 10-, 20-, 30- and 40% of maximal voluntary contraction (MVC). Each workload was 2 min, with brachial artery Doppler ultrasound and DCS-derived BFI being simultaneously assessed. Pearson correlation coefficient revealed a strong relationship ($r = 0.96$, $P < 0.001$) between the two approaches (Fig. 2).

Forearm tissue oxygenation.—Directly measured forearm S_{vO_2} and NIRS-measured tissue oxygen saturation (S_{tO_2}) shared the same directional change with exercise: S_{vO_2} decreased 24.4 ± 3.2% during handgrip (HG) exercise (rest: 61.2 ± 2.9%, exercise: 36.8 ± 1.8%, <0.001, Fig. 1C); NIRS-measured S_{tO_2} decreased 9.4 ± 1.6% ($P<0.001$, Fig. 1D).

The changes in tissue oxygen saturation were driven by increases in deoxyhaemoglobin (rest: 23.2 ± 1.5 μM, exercise: 32.4 ± 2.1 μM, $P<0.001$) and reductions in oxyhaemoglobin (rest: 62.1 ± 2.0 μM, exercise: 56.8 ± 3.2 μM, $P=0.008$).

Forearm $m\dot{V}_{O_2}$ and MRO_2.—As above, Fick-derived $m\dot{V}_{O_2}$ and NIRS–DCS-derived MRO_2 shared the same directional change with exercise (Fig. 1E and F, Table 2).

Experimental Aim 2

Changes in forearm arterial perfusion pressure.—As expected, arm position had a significant effect on FAPP ($P<0.001$). Relative to the neutral position (83 ± 2 mmHg), lowering the arm below the level of the heart elevated FAPP by 15 ± 3 mmHg (to 98 ± 4 mmHg, $P=0.002$). In contrast, raising it above the level of the heart lowered FAPP by 19 ± 2 mmHg (64 ± 3 mmHg, $P<0.001$). As such, these changes in arm position yielded a 34 ± 4 mmHg difference in FAPP between the above- and below-the-heart arm positions ($P<0.001$) during Experimental Aim 2 (Fig. 3A and B).

Baseline values between arm positions.—For conventional measures, Doppler blood flow and O_2 delivery did not differ by arm position at rest (Table 3). Arterial oxygen content was lower at rest with the arm above (17.8 ± 0.2 ml O_2/100 ml) compared to below the heart (18.5 ± 0.2 ml O_2/100 ml, $P=0.003$) due to differences in resting haemoglobin (below: 13.8 ± 0.2 g/dl, above 13.3 ± 0.2 g/dl, $P=0.002$). Similarly, NIRS-measured S_{tO_2} (below: 74.8 ± 1.5%, above: 72.2 ± 1.7%) was significantly lower with the arm above *versus* below the heart ($P=0.004$, both variables). These differences in baseline tissue saturation by arm position appear to be driven entirely by differences in oxyhaemoglobin (below: 69.7 ± 3.3 μM, above: 62.3 ± 3.4 μM, $P=0.02$), as resting deoxyhaemoglobin did not differ between arm position ($P>0.05$). Mean baseline values for all other physiological variables in the arm below and above positions are presented in Table 3.

Because each baseline measurement was acquired after the arm was in its respective position (i.e. above or below the heart) for at least 10 min, and because BFI measured by DCS is reported as a relative change from baseline, it is possible for baseline changes to affect the interpretation of our exercise results. To address this possibility, on a separate visit, in a subset of individuals ($n=3$), BFI measurements were started with the arm in the neutral position, before passively raising or lowering the arm to its respective position. Similar to the baseline Doppler blood flow measurements reported above, DCS-measured BFI remained unchanged from the neutral position, regardless of arm position ($P=0.37$).

Forearm blood flow and tissue perfusion.—For conventional measures, FBF and O_2 delivery during HG exercise increased to a greater extent with the arm below the heart compared to when it was raised above the heart ($P=0.002$, Fig. 3C, Table 3). In contrast,

DCS-measured BFI increased to the same extent, regardless of arm position (Fig. 3D). With the arm below the heart, the time to reach steady-state was nearly identical between FBF and BFI (27.0 *vs.* 28.8 s, respectively; Fig. 4A and B). When the arm was raised above the heart level, the time to reach steady-state was delayed for both FBF and BFI (32.4 *vs.* 51.0 s, respectively; Fig. 4A and B).

Forearm tissue oxygenation.—Directly measured forearm S_{tO_2} decreased similarly below (−21.7 ± 4.0%) and above (−23.2 ± 3.3%) the level of the heart during HG exercise (Fig. 3E). The NIRS–DCS system also measured similar reductions in S_{tO_2} (below: −5.8 ± 0.8%, above: −5.6 ± 1.3%, Fig. 3F) between arm positions during steady-state (end of) exercise. In both positions, NIRS-measured deoxyhaemoglobin increased similarly during exercise in the below +5.8 ± 0.9 μM and above +6.5 ± 1.7 μM arm positions (time: $P <$ 0.001, interaction: $P = 0.69$). In contrast, the drop in oxyhaemoglobin during exercise in the below position −4.8 ± 1.1 μM was significantly greater compared to the above position −1.3 ± 0.8 μM (time: $P = 0.001$, interaction $P = 0.003$). Importantly, the change in tissue saturation during exercise with the arm above the heart was much faster (55.8 s [95% confidence interval (CI): 33.6, 102.6]) than when the arm was below the heart (124.8 s [95% CI: 72.0, 306.0]), as shown in Fig. 4C.

Forearm $m\dot{V}_{O_2}$ and MRO_2.—Driven by a higher convective oxygen delivery, there was a trend ($P = 0.11$) towards a higher $m\dot{V}_{O_2}$ during HG exercise performed in the below condition (Fig. 3G, Table 3). In contrast, we observed no difference in the increase in NIRS–DCS-measured MRO_2 during HG exercise with the arm below *versus* above the heart ($P =$ 0.65). As observed in Aim 1, both approaches shared the same upward direction of change for $m\dot{V}_{O_2}$ and MRO_2. In addition, the time constants for MRO_2 were similar between the arm below the heart (51.6 s [95% CI: 37.2, 72.0]) and arm above the heart (63.6 s [95% CI: 50.4, 82.2]) conditions (Fig. 4D), despite the prolonged increase in BFI observed with the arm above the heart, which was seemingly compensated for with a faster rate of tissue desaturation (a major advantage of NIRS–DCS over conventional single-point approaches).

Reproducibility of experimental measures

To assess between-day (test–retest) reproducibility of DCS-measured BFI we repeated the same conditions (neutral, below, above arm positions) during a separate (3rd) visit, in one subject. FBF measured by Doppler ultrasound and BFI measured by the NIRS–DCS system during visits 2 and 3 for each arm position are presented in Fig. 5. Both measures (FBF and BFI) demonstrate excellent reproducibility during both the below- and above-the-heart arm positions. Of note, BFI is higher in the neutral position during exercise in the 3rd compared to the 2nd visit; however, this is in agreement with higher conduit flow measured by Doppler ultrasound during the respective visits.

Discussion

The major novel findings of this investigation are threefold. First, during exercise in the neutral position, we found good concurrent validity between conventional and NIRS–DCS-

derived measures of: (a) convective oxygen delivery (Doppler-derived FBF *versus* DCS-derived BFI), (b) oxygen utilization (S_{vO_2} *versus* NIRS-derived tissue saturation). Second, by experimentally manipulating forearm arterial perfusion pressure, we uncoupled convective oxygen delivery from microvascular perfusion, highlighting previously unattainable differences between these two measures during steady-state exercise. Third, and perhaps most importantly, because NIRS–DCS provides nearly continuous measurements of oxygen delivery and utilization throughout exercise, we were able to observe a unique interplay between oxygen delivery and utilization when forearm perfusion pressure was manipulated. Specifically, our data show that when steady-state microvascular perfusion is delayed (with the arm exercising above the heart), oxygen extraction compensates (accelerated tissue desaturation), preserving skeletal muscle oxygen consumption. Taken together, these data support a novel role for DCS in understanding the determinants of oxygen consumption in exercising muscle at the microvascular level and hold great promise for future clinical application.

Experimental Aim 1

While DCS is rapidly gaining popularity as a novel, non-invasive tool for assessing local microvascular perfusion, application of DCS to exercising muscle remains limited (Gurley *et al.* 2012; Shang *et al.* 2013; Carp *et al.* 2017; Hammer *et al.* 2018). Moreover, validation of DCS against conventional measures of convective oxygen delivery – in exercising skeletal muscle – is also limited. In fact, to our knowledge, we have been the only lab to address this knowledge gap (Bangalore-Yogananda *et al.* 2018), showing excellent agreement between DCS-derived blood flow index and Doppler-derived brachial artery blood flow during rhythmic handgrip exercise. The current data confirm and extend these prior observations in two important ways. First, we show good concurrent validity between Doppler-derived blood flow and DCS-derived blood flow index during rhythmic handgrip exercise, during exercise at a fixed-workload. Second, we show a strong relationship between Doppler ultrasound and DCS-derived BFI across a greater range of exercise intensities than previously evaluated (Fig. 2).

Near-infrared spectroscopy is an established technique for characterizing the transport and utilization of oxygen through the microcirculation (Belardinelli *et al.* 1995; DeLorey *et al.* 2003, 2004; Grassi *et al.* 2003; Ferreira *et al.* 2005; Broxterman *et al.* 2014, 2015; Koga *et al.* 2014; Grassi & Quaresima, 2016; Sun *et al.* 2016; Barstow, 2019). That tissue saturation declined with rhythmic handgrip exercise between 20 and 30% MVC is entirely consistent with several previous investigations (Boushel *et al.* 1998; Hicks *et al.* 1999; Gurley *et al.* 2012; Hammer *et al.* 2018). That the decline in tissue saturation was directionally similar to the measured venous oxygen saturation change is also consistent with several previous observations (Wilson *et al.* 1989; Mancini *et al.* 1994; Boushel *et al.* 1998; Hicks *et al.* 1999; Sun *et al.* 2016). As intriguing as these directional similarities are, however, we are aware that these two indices do not represent the same thing. Specifically, oxygen saturation measured in the venous effluent represents ‘pure’ oxygen extraction across the whole muscle. In contrast, tissue saturation represents a balance between arterial input and muscle oxygen extraction. By coupling tissue saturation with novel DCS-derived microvascular

perfusion, we believe the determinants of oxygen consumption, and the mechanism(s) of exercise intolerance, may be better understood.

Experimental Aim 2

To explore the utility of NIRS–DCS across the physiological spectrum, we altered forearm perfusion pressure by changing the position of the arm above or below the heart. This approach has been used previously with good success (Saunders & Tschakovsky, 2004; Tschakovsky *et al.* 2004; Walker *et al.* 2007; Bentley *et al.* 2014; Jasperse *et al.* 2015), showing remarkably similar responses in Doppler-derived brachial artery blood flow to those found in this investigation. Contrary to our hypothesis, however, steady-state DCS-derived microvascular BFI did not differ between arm positions, suggesting that in healthy young adults, muscle perfusion is closely matched to metabolic demand, regardless of conduit blood flow or perfusion pressure. We interpret this finding to reflect myogenic autoregulation, whereby the microvasculature is compensating to maintain oxygen delivery to the exercising muscle by redistributing available blood to the working skeletal muscle. This is further supported by the similar changes in both tissue saturation and venous saturation between the two arm positions at the end of exercise, suggesting that when muscle perfusion is matched (despite a marked time delay), and when metabolic demand is held constant (i.e. 13 kg), muscle oxygen consumption is similar.

It cannot be overlooked, however, that we also observed marked differences in oxygen delivery and utilization at the onset of exercise. Indeed, we observed a consistent temporal ‘lag’ in skeletal muscle perfusion with the arm exercising above the heart, supporting the effectiveness of our experimental model. Remarkably, this delay in skeletal muscle perfusion was compensated for by changes in oxygen extraction, as evidenced by the observed acceleration in tissue desaturation. As a result, skeletal muscle oxygen consumption was closely matched, between arm positions, across the entire exercise bout, regardless of convective oxygen delivery or perfusion pressure. These data highlight two important points. First, the nearly continuous nature of NIRS–DCS measurements provides insight beyond conventional Fick determinants of muscle oxygen consumption. Second, the data here establish strong proof-of-concept, supporting a future role of NIRS–DCS in differentiating pathophysiological mechanisms contributing to exercise intolerance in clinical populations with impaired oxygen delivery to and/or utilization by the active muscles.

Limitations

This study is not without limitation. The NIRS–DCS probe was placed by an experienced investigator, with every effort made to centre the probe over the belly of the flexor digitorum profundus. This is, however, a small muscle, with multiple neighbouring muscle groups, and thus we cannot rule out the possibility of competing signals from neighbouring tissues. In our hands, however, failure to centre the probe directly over skeletal muscle results in tremendous noise in the data. While our data suggest a tight relationship between Doppler-derived FBF and DCS-derived BFI during moderate-intensity small muscle mass exercise performed in the neutral condition, differences may exist between conduit artery and microcirculatory blood flow kinetics particularly in larger muscle mass exercise (Harper *et al.* 2006) or higher intensity exercise (Hammer *et al.* 2018). In addition, others have shown

that regional differences in muscle oxygen utilization exist during large muscle mass exercise (Vogiatzis *et al.* 2015), which may have influenced the present NIRS–DCS results and need to be considered in future applications of this technology. Moreover, caution is indeed warranted when interpreting the current kinetics data, as only one baseline to exercise transition was performed for these initial proof-of-concept experiments (Grassi *et al.* 2003). Finally, we did not account for potential differences in mean transit time from capillaries to venous sampling, which is necessary to achieve the most accurate match between muscle blood flow and oxygen extraction for the $m\dot{V}_{O_2}$ calculation (Bangsbo *et al.* 2000).

Because DCS operates under the same principles as NIRS, it shares similar technical susceptibilities. For example, changes in skin blood flow have indeed been shown to influence NIRS-derived oxyhaemoglobin content (Davis *et al.* 2006; Tew *et al.* 2010). Given that we performed small muscle mass exercise, for a brief period of time, in a thermoneutral environment, gives us great confidence that our signal was not influenced by changes in skin blood flow. The relative contributions of arterioles, capillaries and venules to the optical signal during handgrip exercise at ~25% MVC is unclear. However, it should be noted that capillaries comprise the majority of skeletal muscle microvascular volume (Poole *et al.* 1995; Hammer *et al.* 2018). As such, it can be inferred that changes in optical signal strength observed during exercise likely represent changes in O_2 transportation measurements at the level of the microcirculation (Lutjemeier *et al.* 2008). Lastly, the strength of optical spectroscopic signals in NIRS–DCS may also be influenced by excess subcutaneous fat (van Beekvelt *et al.* 2001; Bopp *et al.* 2011). However, we do not believe this affected our results, given that the flexor digitorum profundus muscle is already very superficial, and forearm skin fold thickness was very low in our young, healthy subjects. Furthermore, since each subject performed all experimental conditions, differences in adipose tissue thickness across subjects are unlikely to influence statistical outcomes as comparisons are primarily within-subject.

Clinical implications

Unlike conventional near-infrared spectroscopy (NIRS), which measures relative concentrations of oxygenated and deoxygenated haemoglobin at two or more wavelengths, DCS provides an index of microvascular perfusion based on subtle intensity fluctuations of diffused monochromatic light. Combining DCS with conventional NIRS introduces exciting new possibilities for better understanding the determinants of skeletal muscle oxygen consumption and for defining the mechanisms driving exercise intolerance. This latter opportunity could help to establish novel therapeutic targets and promote precision-based medicine. More studies, like the one described here, aimed at validating this new approach are therefore critical to the evolution of this new technology, as we seek to fully define its strengths and limitations. DCS data have, however, been extremely promising to-date, supporting the potential for rapid translation of this technology to clinical studies.

In conclusion, the data herein establish good concurrent validity between NIRS–DCS and conventional measures of oxygen delivery and utilization, but raise important questions about their relatedness across the physiological spectrum. Specifically, in contrast to the Fick determinants of $m\dot{V}_{O_2}$ which suggest that the lower $m\dot{V}_{O_2}$ during HG ‘above’ is driven

primarily by a lower convective oxygen delivery, our data suggest that microvascular perfusion is matched to metabolic demand, regardless of changes in conduit blood flow or perfusion pressure (i.e. myogenic autoregulation). Moreover, the data show that any temporal changes in muscle perfusion are compensated for with accelerated oxygen extraction, preserving muscle $\dot{V}_{O_2}$ across the exercise bout. Taken together, these data support a novel role for DCS in understanding the determinants of oxygen consumption in exercising muscle at the microvascular level, and establish good proof-of-concept for NIRS–DCS to provide novel pathophysiological insight across the health and cardiovascular disease continuum.

Acknowledgements

The authors appreciate the time and effort put in by all research subjects. We also wish to thank Drs Craig G. Crandall (University of Texas Southwestern Medical Centre) and Dr Richard Thompson (University of Alberta) for their constructive feedback on the interpretation of these data.

Funding

This research was funded by a University of Texas at Arlington Nagy Family Endowment Award (M.D.N.) and a National Institutes of Health (NIH) grant: R15 HL140989-01 (M.D.N.). W. J. Tucker is financially supported by the American Heart Association (AHA; Postdoctoral Fellowship Grant: 18POST33990210). M. J. Haykowsky is financially supported by the Moritz Chair in Geriatrics at the University of Texas at Arlington.

Biography

Wesley J. Tucker received his PhD in Physical Activity, Nutrition and Wellness from Arizona State University in 2016.He is currently a postdoctoral fellow training in both Dr Michael Nelson's Applied Physiology and Advanced Imaging Laboratory, and Dr Mark Haykowsky's Integrated Cardiovascular Exercise Physiology and Rehabilitation Laboratory at the University of Texas at Arlington. Dr Tucker's research interests include investigating the central and peripheral mechanisms responsible for exercise intolerance across the heart failure continuum, and the efficacy of novel diet- and exercise-based interventions to improve cardiovascular-related health outcomes.

References

Baker WB, Li Z, Schenkel SS, Chandra M, Busch DR, Englund EK, Schmitz KH, Yodh AG, Floyd TF & Mohler ER 3rd (2017). Effects of exercise training on calf muscle oxygen extraction and blood flow in patients with peripheral artery disease. J Appl Physiol (1985) 123, 1599–1609. [PubMed: 28982943]

Bangalore-Yogananda CG, Rosenberry R, Soni S, Liu H, Nelson MD & Tian F (2018). Concurrent measurement of skeletal muscle blood flow during exercise with diffuse correlation spectroscopy and Doppler ultrasound. Biomed Opt Express 9, 131–141. [PubMed: 29359092]

Bangsbo J, Krustrup P, Gonzalez-Alonso J, Boushel R & Saltin B (2000). Muscle oxygen kinetics at onset of intense dynamic exercise in humans. Am J Physiol Regul Integr Comp Physiol 279, R899–R906. [PubMed: 10956247]

Barstow TJ (2019). CORP: Understanding near infrared spectroscopy (NIRS) and its application to skeletal muscle research. J Appl Physiol (1985) (in press; 10.1152/japplphysiol.00166.2018).

Belardinelli R, Barstow TJ, Porszasz J & Wasserman K (1995). Changes in skeletal muscle oxygenation during incremental exercise measured with near infrared spectroscopy. Eur J Appl Physiol Occup Physiol 70, 487–492. [PubMed: 7556120]

Bentley RF, Kellawan JM, Moynes JS, Poitras VJ, Walsh JJ & Tschakovsky ME (2014). Individual susceptibility to hypoperfusion and reductions in exercise performance when perfusion pressure is reduced: evidence for vasodilator phenotypes. J Appl Physiol (1985) 117, 392–405. [PubMed: 24970851]

Bi R, Dong J, Poh CL & Lee K (2015). Optical methods for blood perfusion measurement – theoretical comparison among four different modalities. J Opt Soc Am A Opt Image Sci Vis 32, 860–866. [PubMed: 26366910]

Boas DA, Strangman G, Culver JP, Hoge RD, Jasdzewski G, Poldrack RA, Rosen BR & Mandeville JB (2003). Can the cerebral metabolic rate of oxygen be estimated with near-infrared spectroscopy? Phys Med Biol 48, 2405–2418. [PubMed: 12953906]

Bopp CM, Townsend DK & Barstow TJ (2011). Characterizing near-infrared spectroscopy responses to forearm post-occlusive reactive hyperemia in healthy subjects. Eur J Appl Physiol 111, 2753–2761. [PubMed: 21409404]

Boushel R, Pott F, Madsen P, Radegran G, Nowak M, Quistorff B & Secher N (1998). Muscle metabolism from near infrared spectroscopy during rhythmic handgrip in humans. Eur J Appl Physiol Occup Physiol 79, 41–48. [PubMed: 10052659]

Broxterman RM, Ade CJ, Wilcox SL, Schlup SJ, Craig JC & Barstow TJ (2014). Influence of duty cycle on the power-duration relationship: observations and potential mechanisms. Respir Physiol Neurobiol 192, 102–111. [PubMed: 24361503]

Broxterman RM, Craig JC, Smith JR, Wilcox SL, Jia C, Warren S & Barstow TJ (2015). Influence of blood flow occlusion on the development of peripheral and central fatigue during small muscle mass handgrip exercise. J Physiol 593, 4043–4054. [PubMed: 26104881]

Carp SA, Farzam P, Redes N, Hueber DM & Franceschini MA (2017). Combined multi-distance frequency domain and diffuse correlation spectroscopy system with simultaneous data acquisition and real-time analysis. Biomed Opt Express 8, 3993–4006. [PubMed: 29026684]

Cope M, Delpy DT, Reynolds EO, Wray S, Wyatt J & van der Zee P (1988). Methods of quantitating cerebral near infrared spectroscopy data. Adv Exp Med Biol 222, 183–189. [PubMed: 3129910]

Davis SL, Fadel PJ, Cui J, Thomas GD & Crandall CG (2006). Skin blood flow influences near-infrared spectroscopy-derived measurements of tissue oxygenation during heat stress. J Appl Physiol (1985) 100, 221–224. [PubMed: 16150842]

DeLorey DS, Kowalchuk JM & Paterson DH (2003). Relationship between pulmonary O_2 uptake kinetics and muscle deoxygenation during moderate-intensity exercise. J Appl Physiol (1985) 95, 113–120. [PubMed: 12679363]

DeLorey DS, Kowalchuk JM & Paterson DH (2004). Effects of prior heavy-intensity exercise on pulmonary O_2 uptake and muscle deoxygenation kinetics in young and older adult humans. J Appl Physiol (1985) 97, 998–1005. [PubMed: 15133009]

Dong J, Bi R, Ho JH, Thong PS, Soo KC & Lee K (2012). Diffuse correlation spectroscopy with a fast Fourier transform-based software autocorrelator. J Biomed Opt 17, 097004.

Ferreira LF, Townsend DK, Lutjemeier BJ & Barstow TJ (2005). Muscle capillary blood flow kinetics estimated from pulmonary O_2 uptake and near-infrared spectroscopy. J Appl Physiol (1985) 98, 1820–1828. [PubMed: 15640391]

Grassi B, Pogliaghi S, Rampichini S, Quaresima V, Ferrari M, Marconi C & Cerretelli P (2003). Muscle oxygenation and pulmonary gas exchange kinetics during cycling exercise on-transitions in humans. J Appl Physiol (1985) 95, 149–158. [PubMed: 12611769]

Grassi B & Quaresima V (2016). Near-infrared spectroscopy and skeletal muscle oxidative function in vivo in health and disease: a review from an exercise physiology perspective. J Biomed Opt 21, 091313. [PubMed: 27443955]

Gurley K, Shang Y & Yu G (2012). Noninvasive optical quantification of absolute blood flow, blood oxygenation, and oxygen consumption rate in exercising skeletal muscle. J Biomed Opt 17, 075010. [PubMed: 22894482]

Hammer SM, Alexander AM, Didier KD, Smith JR, Caldwell JT, Sutterfield SL, Ade CJ & Barstow TJ (2018). The noninvasive simultaneous measurement of tissue oxygenation and microvascular hemodynamics during incremental handgrip exercise. J Appl Physiol (1985) 124, 604–614. [PubMed: 29357515]

Harper AJ, Ferreira LF, Lutjemeier BJ, Townsend DK & Barstow TJ (2006). Human femoral artery and estimated muscle capillary blood flow kinetics following the onset of exercise. Exp Physiol 91, 661–671. [PubMed: 16556660]

Henry B, Zhao M, Shang Y, Uhl T, Thomas DT, Xenos ES, Saha SP & Yu G (2015). Hybrid diffuse optical techniques for continuous hemodynamic measurement in gastrocnemius during plantar flexion exercise. J Biomed Opt 20, 125006. [PubMed: 26720871]

Herr MD, Hogeman CS, Koch DW, Krishnan A, Momen A & Leuenberger UA (2010). A real-time device for converting Doppler ultrasound audio signals into fluid flow velocity. Am J Physiol Heart Circ Physiol 298, H1626–H1632. [PubMed: 20173048]

Hicks A, McGill S & Hughson RL (1999). Tissue oxygenation by near-infrared spectroscopy and muscle blood flow during isometric contractions of the forearm. Can J Appl Physiol 24, 216–230. [PubMed: 10364417]

Jasperse JL, Shoemaker JK, Gray EJ & Clifford PS (2015). Positional differences in reactive hyperemia provide insight into initial phase of exercise hyperemia. J Appl Physiol (1985) 119, 569–575. [PubMed: 26139221]

Kiernan M, Schoffman DE, Lee K, Brown SD, Fair JM, Perri MG & Haskell WL (2013). The Stanford Leisure-Time Activity Categorical Item (L-Cat): a single categorical item sensitive to physical activity changes in overweight/obese women. Int J Obes (Lond) 37, 1597–1602. [PubMed: 23588625]

Kim MN, Edlow BL, Durduran T, Frangos S, Mesquita RC, Levine JM, Greenberg JH, Yodh AG & Detre JA (2014). Continuous optical monitoring of cerebral hemodynamics during head-of-bed manipulation in brain-injured adults. Neurocrit Care 20, 443–453. [PubMed: 23653267]

Koga S, Rossiter HB, Heinonen I, Musch TI & Poole DC (2014). Dynamic heterogeneity of exercising muscle blood flow and O_2 utilization. Med Sci Sports Exerc 46, 860–876. [PubMed: 24091989]

Lutjemeier BJ, Ferreira LF, Poole DC, Townsend D & Barstow TJ (2008). Muscle microvascular hemoglobin concentration and oxygenation within the contraction-relaxation cycle. Respir Physiol Neurobiol 160, 131–138. [PubMed: 17964228]

Mancini DM, Bolinger L, Li H, Kendrick K, Chance B & Wilson JR (1994). Validation of near-infrared spectroscopy in humans. J Appl Physiol (1985) 77, 2740–2747. [PubMed: 7896615]

Poole DC, Wagner PD & Wilson DF (1995). Diaphragm microvascular plasma PO2 measured in vivo. J Appl Physiol (1985) 79, 2050–2057. [PubMed: 8847273]

Ross KM, Leahey TM & Kiernan M (2018). Validation of the Stanford Leisure-Time Activity Categorical Item (L-Cat) using armband activity monitor data. Obes Sci Pract 4, 276–282. [PubMed: 29951218]

Saunders NR & Tschakovsky ME (2004). Evidence for a rapid vasodilatory contribution to immediate hyperemia in rest-to-mild and mild-to-moderate forearm exercise transitions in humans. J Appl Physiol (1985) 97, 1143–1151. [PubMed: 15155716]

Shang Y, Chen L, Toborek M & Yu G (2011). Diffuse optical monitoring of repeated cerebral ischemia in mice. Opt Express 19, 20301–20315. [PubMed: 21997041]

Shang Y, Gurley K & Yu G (2013). Diffuse correlation spectroscopy (DCS) for assessment of tissue blood flow in skeletal muscle: recent progress. Anat Physiol 3, 128. [PubMed: 24724043]

Shang Y, Li T & Yu G (2017). Clinical applications of near-infrared diffuse correlation spectroscopy and tomography for tissue blood flow monitoring and imaging. Physiol Meas 38, R1. [PubMed: 28199219]

Sun YI, Ferguson BS, Rogatzki MJ, McDonald JR & Gladden LB (2016). Muscle near-infrared spectroscopy signals versus venous blood hemoglobin oxygen saturation in skeletal muscle. Med Sci Sports Exerc 48, 2013–2020. [PubMed: 27635772]

Tew GA, Ruddock AD & Saxton JM (2010). Skin blood flow differentially affects near-infrared spectroscopy-derived measures of muscle oxygen saturation and blood volume at rest and during dynamic leg exercise. Eur J Appl Physiol 110, 1083–1089. [PubMed: 20700602]

Tschakovsky ME, Rogers AM, Pyke KE, Saunders NR, Glenn N, Lee SJ, Weissgerber T & Dwyer EM (2004). Immediate exercise hyperemia in humans is contraction intensity dependent: evidence for rapid vasodilation. J Appl Physiol (1985) 96, 639–644. [PubMed: 14578368]

van Beekvelt MC, Borghuis MS, van Engelen BG, Wevers RA & Colier WN (2001). Adipose tissue thickness affects in vivo quantitative near-IR spectroscopy in human skeletal muscle. Clin Sci (Lond) 101, 21–28. [PubMed: 11410110]

Vogiatzis I, Habazettl H, Louvaris Z, Andrianopoulos V, Wagner H, Zakynthinos S & Wagner PD (2015). A method for assessing heterogeneity of blood flow and metabolism in exercising normal human muscle by near-infrared spectroscopy. J Appl Physiol (1985) 118, 783–793. [PubMed: 25593285]

Walker KL, Saunders NR, Jensen D, Kuk JL, Wong SL, Pyke KE, Dwyer EM & Tschakovsky ME (2007). Do vasoregulatory mechanisms in exercising human muscle compensate for changes in arterial perfusion pressure? Am J Physiol Heart Circ Physiol 293, H2928–H2936. [PubMed: 17704292]

Wilson JR, Mancini DM, McCully K, Ferraro N, Lanoce V & Chance B (1989). Noninvasive detection of skeletal muscle underperfusion with near-infrared spectroscopy in patients with heart failure. Circulation 80, 1668–1674. [PubMed: 2598429]

Yu G, Floyd TF, Durduran T, Zhou C, Wang J, Detre JA & Yodh AG (2007). Validation of diffuse correlation spectroscopy for muscle blood flow with concurrent arterial spin labeled perfusion MRI. Opt Express 15, 1064–1075. [PubMed: 19532334]

Zhou C, Eucker SA, Durduran T, Yu G, Ralston J, Friess SH, Ichord RN, Margulies SS & Yodh AG (2009). Diffuse optical monitoring of hemodynamic changes in piglet brain with closed head injury. J Biomed Opt 14, 034015. [PubMed: 19566308]

Key points

- Diffuse correlation spectroscopy (DCS) is emerging as a powerful tool to assess skeletal muscle perfusion.
- Near-infrared spectroscopy (NIRS) is an established technique for characterizing the transport and utilization of oxygen through the microcirculation.
- Here we compared a combined NIRS–DCS system with conventional measures of oxygen delivery and utilization during handgrip exercise. The data show good concurrent validity between convective oxygen delivery and DCS-derived blood flow index, as well as between oxygen extraction at the conduit and microvascular level.
- We then manipulated forearm arterial perfusion pressure by adjusting the position of the exercising arm relative to the position of the heart. The data show that microvascular perfusion can be uncoupled from convective oxygen delivery, and that tissue saturation seemingly compensates to maintain skeletal muscle oxygen consumption.
- Taken together, these data support a novel role for NIRS–DCS in understanding the determinants of muscle oxygen consumption at the microvascular level.

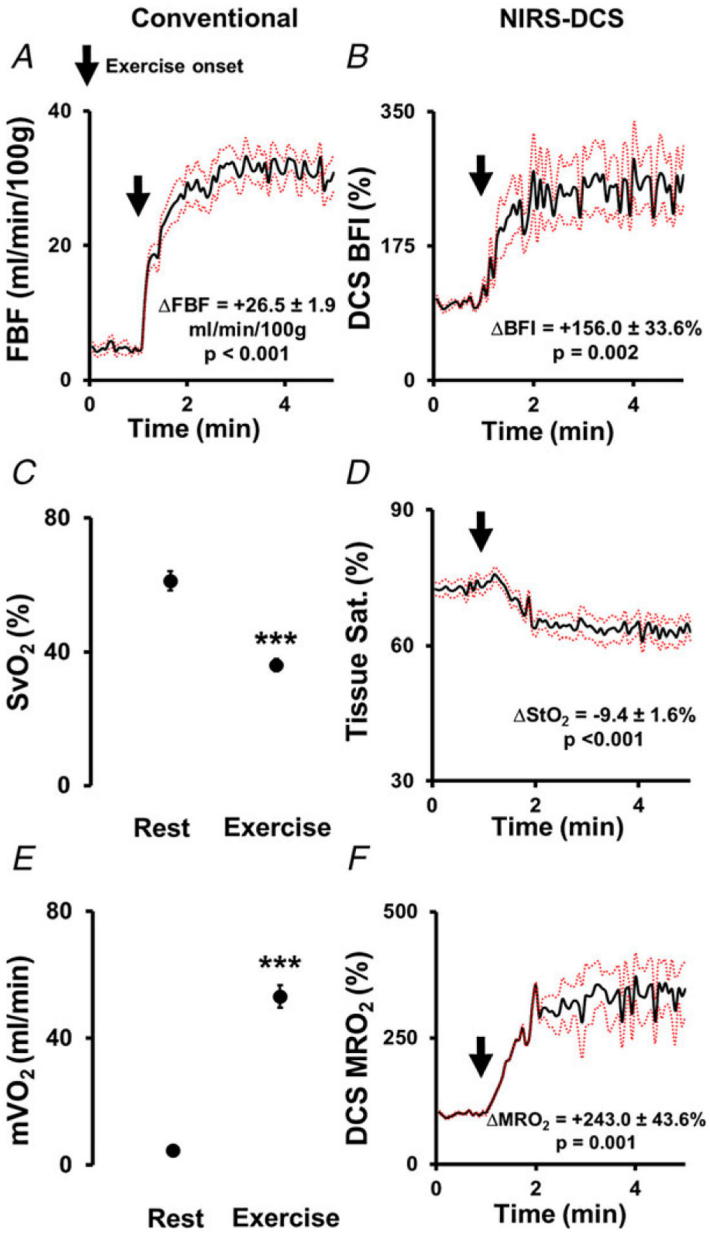

Figure 1. Mean oxygen delivery and utilization responses to 13 kg handgrip exercise assessed by conventional measures (left panels) and non-invasive combined NIRS–DCS system (right panels) at heart level

Blood flow and tissue perfusion responses depicted by Doppler ultrasound-measured forearm blood flow (FBF) indexed to 100 g lean tissue (*A*) and by DCS-derived muscle blood flow index (BFI) (*B*). Muscle oxygen utilization responses measured invasively via venous oxygen saturation (S_{vO_2}) (*C*) and non-invasively via NIRS-derived tissue saturation (S_{tO_2}) (*D*). Skeletal muscle oxygen uptake ($m\dot{V}_{O_2}$) (*E*) and NIRS–DCS-derived muscle relative oxygen uptake (MRO_2) (*F*) represent the measured oxygen cost of muscular work during handgrip exercise. ***$P < 0.001$ compared to rest. $n = 9$. Arrows denote the onset of exercise. Data reported as means ± SEM.

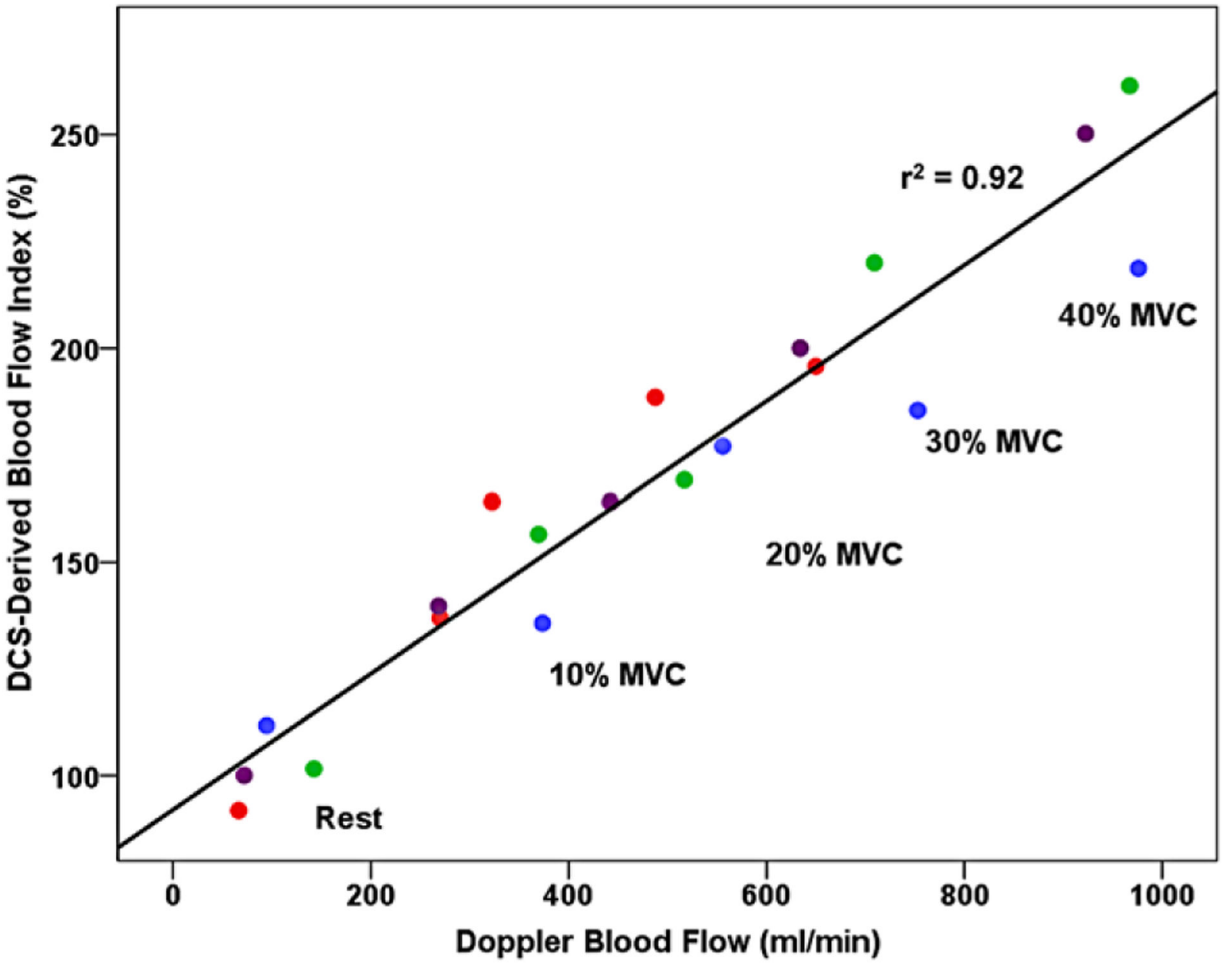

Figure 2. Correlation of Doppler-derived brachial artery blood flow (ml/min) with DCS-derived muscle blood flow index (%)

Measurements taken at baseline, 10-, 20-, 30- and 40% of maximal voluntary contraction (MVC) handgrip exercise. $n = 4$.

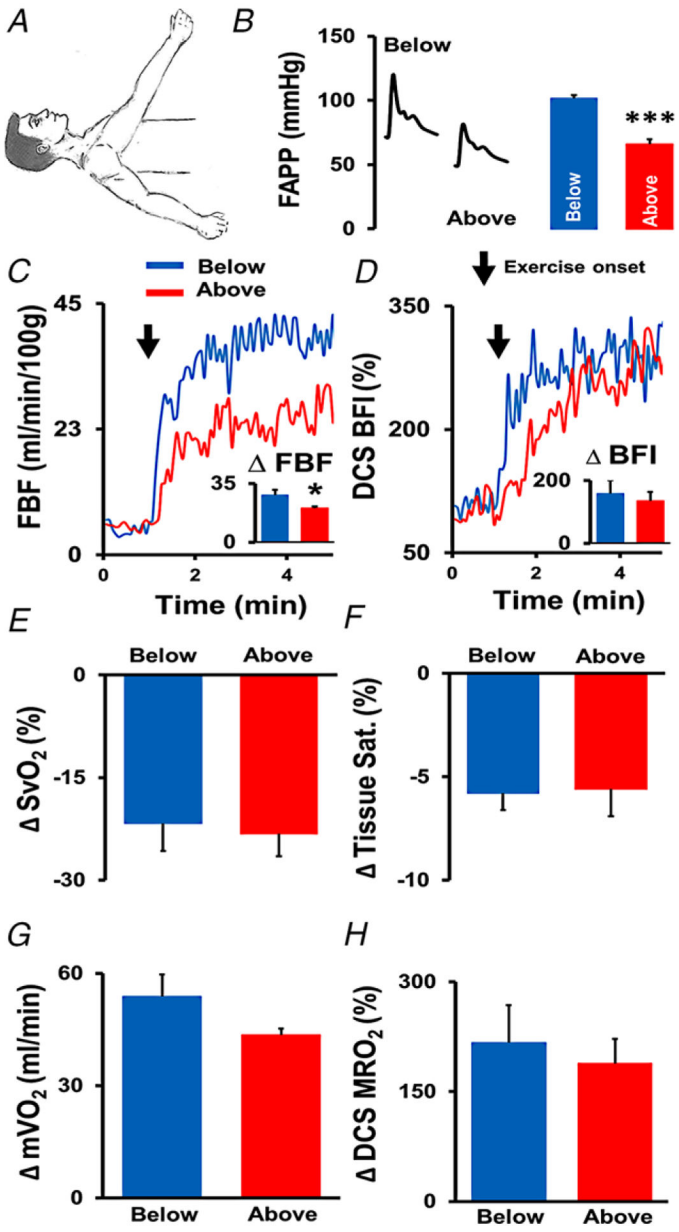

Figure 3. Manipulation of forearm arterial perfusion pressure (FAPP)

The exercising arm was positioned above and below the level of the heart to experimentally manipulate skeletal muscle oxygen delivery (*A* and *B*). Red lines and bars represent the above heart condition, and blue lines and bars represent the below heart condition. *** denotes a significant difference between arm positions ($P < 0.001$). *C*, forearm blood flow indexed to 100 g of lean tissue (measured by Doppler ultrasound) in a representative subject at rest and during exercise, with group mean Δ data (change from rest) displayed in the corresponding figure inset. * denotes a significant difference between arm positions ($P = 0.02$). *D*, microvascular tissue perfusion (measured by DCS-derived blood flow index (BFI)) in the same representative subject at rest and during exercise, with corresponding group mean Δ data (change from rest) in the figure inset. *E*, mean change in venous oxygen

saturation (S_{vO_2}) during exercise in each condition. *F*, mean change in NIRS-derived tissue saturation (S_{tO_2}) during exercise in each condition. *G* and *H*, mean changes in skeletal muscle oxygen uptake ($m\dot{V}_{O_2}$) and NIRS–DCS-derived muscle relative oxygen uptake (MRO_2) during exercise in each condition. $n = 8$. Arrows denote the onset of exercise. Data reported as means ± SEM.

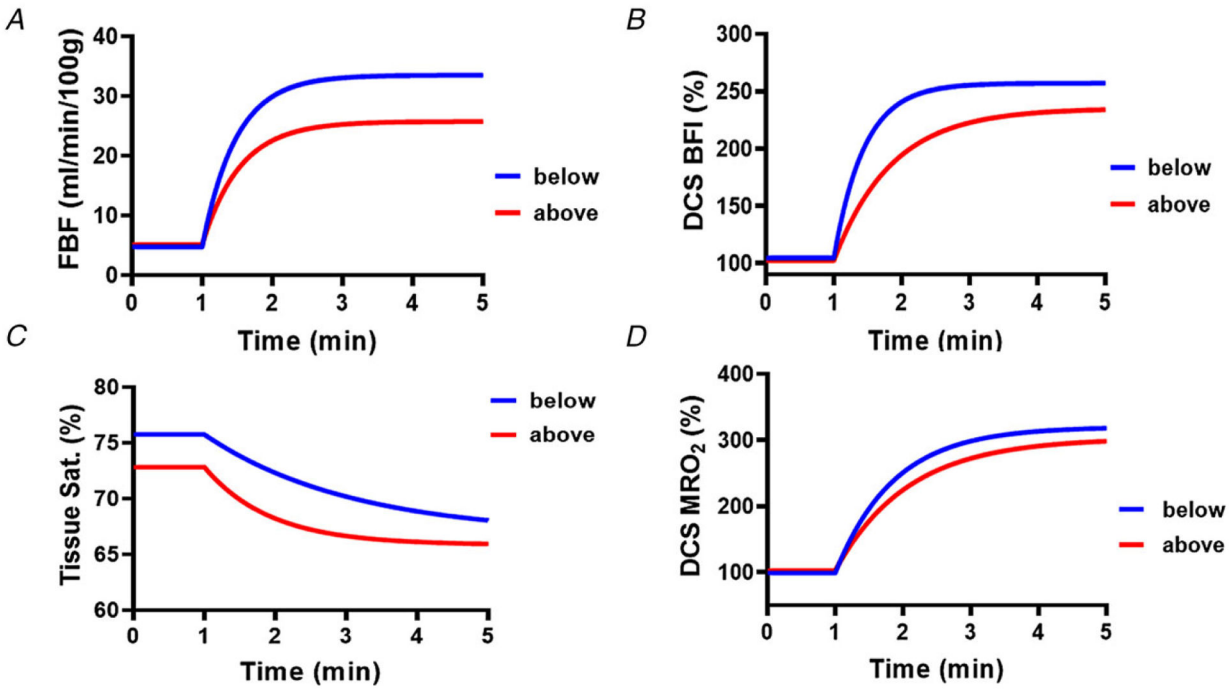

Figure 4. Exercise onset kinetics

Monoexponentially fitted data for Doppler ultrasound-measured forearm blood flow (FBF) indexed to 100 g lean tissue (*A*), DCS-derived muscle blood flow index (BFI) (*B*), NIRS-derived tissue saturation (*C*), and NIRS–DCS-derived muscle relative oxygen uptake (MRO_2) (*D*) with the arm below and above the heart. $n = 8$.

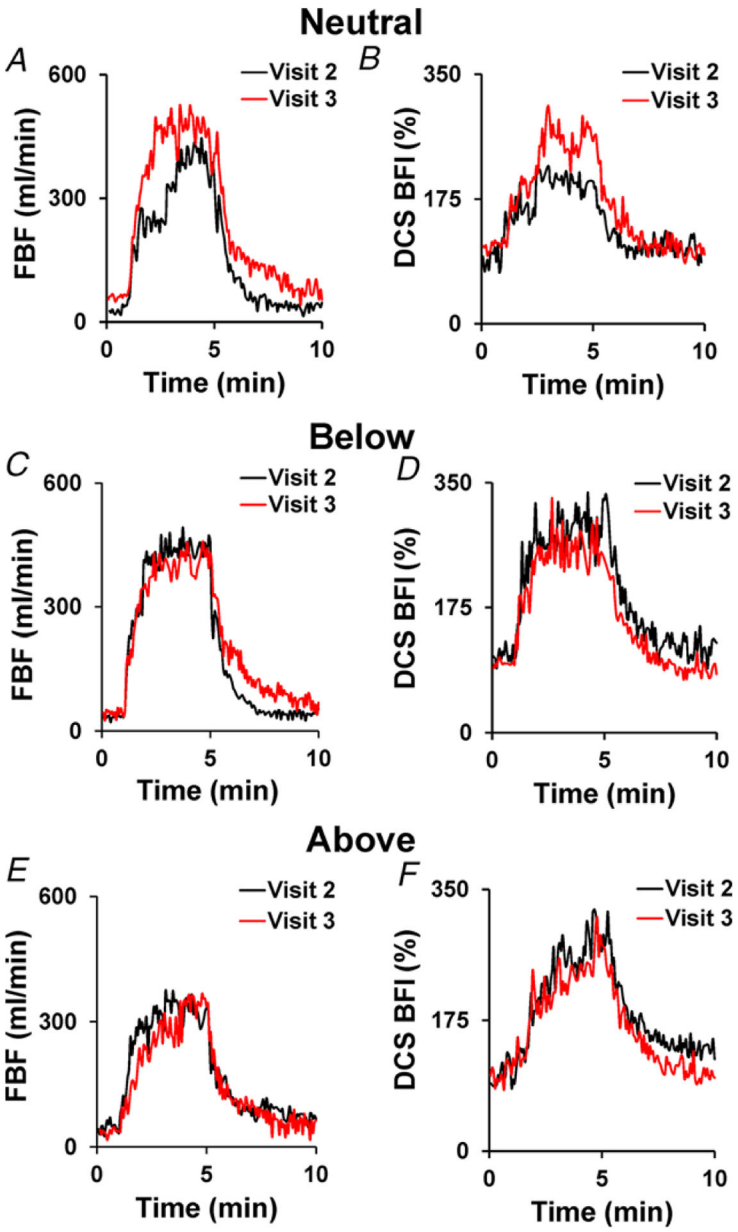

Figure 5. Between-visit reproducibility of Doppler ultrasound-measured forearm blood flow (FBF) and DCS-measured blood flow index (BFI) responses to 13 kg handgrip exercise performed in the neutral (*A* and *B*), below (*C* and *D*) and above the level of the heart arm positions (*E* and *F*) in a single representative subject

n = 1. To be consistent with the other subjects, only data from this individual's second visit was used for group analyses.

Table 1.

Subject descriptives

Variable	Mean ± SD
Age (years)	26 ± 3
Height (cm)	180.2 ± 6.3
Weight (kg)	85.9 ± 15.9
BMI (kg/m^2)	26.3 ± 3.8
Total body fat (%)	22.4 ± 8.0
Left forearm total mass (g)	1639 ± 212
Left forearm lean mass (g)	1512 ± 204
Left forearm adipose tissue thickness (mm)	4 ± 1
Maximal voluntary contraction (MVC) (kg)	52 ± 8
Relative MVC at 13 kg workload (%)	25.4 ± 3.9
Physical Activity L-Cat Score	5 ± 2[a]

$n = 9$.

[a]Data presented as median ± interquartile range.

Table 2.

Baseline and exercise values measured in the neutral position

Variable	Baseline	Exercise
FBF (ml/min)	71.0 ± 10.0	467.8 ± 27.6***
FBF indexed to forearm LBM (ml/min/100g)	4.7 ± 0.6	31.2 ± 2.0***
MAP (mmHg)	84 ± 3	91 ± 4*
FVC ((ml/min) × 100 mmHg)	86 ± 13	518 ± 46***
HR (beats/min)	58 ± 3	64 ± 3*
Haemoglobin (g/dl)	13.6 ± 0.2	13.7 ± 0.3
S_{aO_2} (%)	96.9 ± 0.5	96.9 ± 0.5
C_{aO_2} (ml O_2/100 ml)	18.1 ± 0.2	18.3 ± 0.3
C_{vO_2} (ml O_2/100 ml)	11.4 ± 0.6	6.9 ± 0.3***
a–vO_{2diff} (ml O_2/100 ml)	6.7 ± 0.5	11.4 ± 0.5***
$m\dot{V}_{O_2}$ (ml/min)	4.6 ± 0.6	53.2 ± 3.5***
O_2 delivery (ml O_2/min)	13.0 ± 1.9	85.5 ± 4.9***

$n = 9$. FBF: forearm blood flow, LBM: lean body mass, MAP: mean arterial pressure, FVC: forearm vascular conductance, HR: heart rate, S_{aO_2}: arterial oxygen saturation, C_{aO_2}: arterial oxygen content, C_{vO_2}: forearm venous oxygen content, a–vO_{2diff}: arteriovenous oxygen difference, $m\dot{V}_{O_2}$: forearm muscle oxygen consumption. Data are means ± SEM.

*** $P < 0.001$ *versus* baseline.

* $P < 0.05$ *versus* baseline.

Table 3.

Baseline and exercise values measured when the arm is below or above the level of the heart

	Below		Above		Time	Interaction
	Baseline	**Exercise**	**Baseline**	**Exercise**	***P* value**	***P* value**
FBF (ml/min)	76.7 ± 18.2	501.0 ± 51.9	79.8 ± 18.4	386.0 ± 22.7	<0.001	0.02
FBF (ml/min/100 g)	4.9 ± 0.9	33.1 ± 3.1	5.1 ± 0.9	25.5 ± 0.8	<0.001	0.02
MAP (mmHg)	87 ± 3	92 ± 5	91 ± 4	100 ± 6	0.001	0.30
FVC ((ml/min) × 100 mmHg)	89 ± 21	552 ± 68	88 ± 22	389 ± 29	<0.001	0.02
HR (beats/min)	55 ± 3	60 ± 3	56 ± 3	63 ± 3	<0.001	0.26
Haemoglobin (g/dl)	13.8 ± 0.2	13.9 ± 0.2	13.3 ± 0.2	13.8 ± 0.2	<0.001	0.01
S_{aO_2} (%)	96.8 ± 0.8	97.2 ± 0.5	96.7 ± 0.7	97.2 ± 0.5	0.08	0.82
C_{aO_2} (ml O_2/100 ml)	18.5 ± 0.2	18.7 ± 0.3	17.8 ± 0.2	18.5 ± 0.2	<0.001	0.01
C_{vO_2} (ml O_2/100 ml)	11.1 ± 1.0	6.9 ± 0.3	9.6 ± 0.8	5.5 ± 0.3	<0.001	0.95
a–vO_{2diff} (ml O_2/100 ml)	7.4 ± 0.9	11.8 ± 0.3	8.2 ± 0.7	13.0 ± 0.3	<0.001	0.69
$m\dot{V}_{O_2}$ (ml/min)	4.8 ± 0.5	58.7 ± 6.0	6.1 ± 1.0	49.7 ± 2.1	<0.001	0.11
O_2 delivery (ml O_2/min)	14.3 ± 3.5	93.8 ± 10.1	14.2 ± 3.3	71.3 ± 3.9	<0.001	0.02

n = 8. FBF: forearm blood flow, LBM: lean body mass, MAP: mean arterial pressure, FVC: forearm vascular conductance, HR: heart rate, S_{aO_2}: arterial oxygen saturation, C_{aO_2}: arterial oxygen content, C_{vO_2}: forearm venous oxygen content, a–vO_{2diff}: arteriovenous oxygen difference, $m\dot{V}_{O_2}$: forearm muscle oxygen consumption. Data are means ± SEM.